Modeling of Aggregation Kernel Using Monte Carlo Simulations of Spray Fluidized Bed Agglomeration

Mubashir Hussain, Mirko Peglow, and Evangelos Tsotsas
Chair of Thermal Process Engineering, Otto-von-Guericke University, Universitätsplatz 2, D-39106 Magdeburg, Germany

Jitendra Kumar
Chair of Thermal Process Engineering, Otto-von-Guericke University, Universitätsplatz 2, D-39106 Magdeburg, Germany

Dept. of Mathematics, Indian Institute of Technology Kharagpur, Kharagpur 721302, West Bengal, India

DOI 10.1002/aic.14332
Published online January 7, 2014 in Wiley Online Library (wileyonlinelibrary.com)

The present work attempts to consider the microscopic mechanisms of spray fluidized bed agglomeration while modeling the macroscopic kinetics of the process. A microscale approach, constant volume Monte-Carlo simulation, is used to analyze the effects of micro-processes on the aggregation behavior and identify the influencing parameters. The identified variables, namely the number of wet particles, the total number of particles, and the number of droplets are modeled and combined in the form of an aggregation kernel. The proposed kernel is then used in a one-dimensional population balance equation for predicting the particle number density distribution. The only fitting parameters remaining in the population balance system are the collision frequency per particle and a success fraction accounting for the dissipation of kinetic energy. Predictions of the population balance model are compared with the results of Monte-Carlo simulations for a variation of significant operating parameters and found to be in good agreement. © 2014 American Institute of Chemical Engineers *AIChE J*, 60: 855–868, 2014

Keywords: computer simulations (MC and MD), mathematical modeling, population balances, aggregation kernel, multiscale modeling

Introduction

Micro-interactions play a fundamental role in molding the macroscopic behavior of processes involving a dispersed system, such as spray fluidized bed granulation (SFBG). In SFBG, particles get aggregated and dried simultaneously by passing through many complex micro-processes which change the physical properties of the particles such as flowability, density or porosity, shape, and so forth. The present work addresses the study of such micro-interactions through a microscale modeling approach and translating their effects onto a macroscale level by modeling the parameters that influence the process.

Many mechanisms such as aggregation, breakage, growth, nucleation, and so forth, might take place during granulation in spray fluidized bed. However, the focus of this work is to correlate the effect of process parameters with the aggregation kinetics and, therefore, all mechanisms except agglomeration have been neglected. Pure agglomeration is not only considered for simplicity but also justified for spray fluidized bed because when aiming at agglomeration, materials, and operating conditions are, in practice, chosen as to avoid all other mechanisms. Besides its extensive application to fluidized bed granulation,[1–3] pure agglomeration has also been assumed, for example, in modeling of drum granulation,[4,5] aerosol dynamics,[6] and crystallization.[7]

The one-dimensional (1-D) population balance equation (PBE) for pure agglomeration in a batch system (also called Smoluchowski equation) using volume of the particle as an internal coordinate is given by, for example, Hulburt and Katz[8] as

$$\frac{\partial n(v,t)}{\partial t} = \frac{1}{2}\int_0^v \beta(t, v-v', v')n(t, v-v')n(t, v')dv' - \int_0^\infty \beta(t, v, v')n(t, v)n(t, v')dv' \tag{1}$$

where v and v' are representations for the volume and β is the aggregation kernel. The PBE is used on a macroscale to predict the particle size distribution (PSD), but this requires prior knowledge of the aggregation kernel $\beta(t, v, v')$.

The aggregation kernel $\beta(t, v, v')$ is usually written as a product of two factors: size-independent term (aggregation efficiency) $\beta_0(t)$ and size-dependent term $\beta^*(v, v')$[1,9–11]

$$\beta(t, v, v') = \beta_0(t)\beta^*(v, v') \tag{2}$$

The aggregation efficiency depends on the operating conditions, moisture distribution, dissipation of kinetic energy,

Correspondence concerning this article should be addressed to M. Hussain at mubashir.hussain@st.ovgu.de.

binder properties, collision orientations, and so forth, can be interpreted as the probability of two colliding particles to form a new agglomerate. The size-independent term $\beta_0(t)$ may further be partitioned to model the fraction of successful collisions.[12] The size-dependent part of the aggregation kernel $\beta^*(v,v')$, on the other hand, reflects the influence of the flow field on the probability of collision between particles of different sizes. Many structures for the aggregation kernel have been presented in literature based on empirical,[1,13] semiempirical,[10,14] and physical[3,15,16] approaches, but a comprehensive model capable of reflecting the effect of process conditions on aggregation behavior under rather general conditions is not yet available. Furthermore, the aggregation efficiency $\beta_0(t)$ is often found to be strongly time dependent when extracted from experimental data. This makes it difficult to correlate $\beta_0(t)$ with the process parameters.

The present work extends the recent work of Hussain et al.[17] to model the aggregation efficiency $\beta_0(t)$ and consequently the parameters affecting $\beta_0(t)$ by mimicking the consideration of micro-processes in Monte-Carlo (MC) simulations. The present work differs in many ways from the previous work of Hussain et al.[17] In this work, we have utilized a comprehensive constant volume MC (CVMC) model of Terrazas-Velarde et al.[18–20] to analyze the effect of micro-processes on the aggregation behavior, whereas in the previous work, a very simplified version of constant number MC (CNMC) was used. Furthermore, the submodel for prediction of the total number of wet particles $\left(N_{\mathrm{p,wet}}\right)$ has been rewritten to predict the results under rather general conditions. In addition, a new submodel for predicting the total number of droplets in the system has been introduced. The prediction of total number of droplets is utilized to compute the average wet surface coverage fraction per wet particle during the simulation. A detailed study on the prediction of particle fractional coverage with liquid has recently been presented by Kariuki et al.[21] However, their work refers to a single particle which remains static during the coating process. Whereas, in this study, the effect of several mechanisms, such as agglomeration of particles, drying of droplets, consumption of droplets in aggregation, and so forth, is considered in predicting average wet surface coverage fraction per wet particle. It should be noted that the liquid binder content shows a significant distribution in the course of the aggregation process. However, the effect of distribution of binder or any other variable can only be modeled in 1-D PBE by means of an average value. The incorporation of distribution of any variable in the macromodel would require the use of multidimensional PBE, which is beyond the scope of this work. The value of the drying time τ of a droplet (needed during modeling) is calculated from the model given in Terrazas-Velarde et al.[19] The only fitting parameters remaining in our work are f_c and ψ which are taken to be constants and extracted from the MC simulation. The methodology followed to achieve the goal is to, first, develop models for predicting the behavior of critical parameters and then incorporate all these models in the form of a comprehensive macromodel to forecast the dynamics of SFBG. This idea is summarized in Figure 1.

It is important to mention here that MC methods have been used conventionally for finding the solution of a PBE, which requires prior knowledge of $\beta_0(t)$ and $\beta^*(v,v')$.[22–25] However, our idea is to use the MC method to approximate the real experimental scenario, as a scaled-down virtual

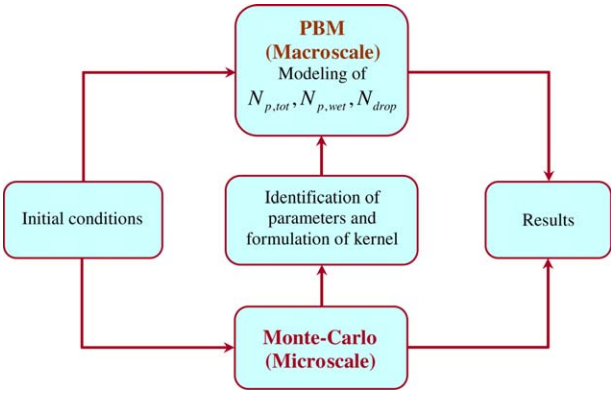

Figure 1. Work flow chart.

[Color figure can be viewed in the online issue, which is available at wileyonlinelibrary.com.]

spray fluidized bed granulator, comparable to the work of Terrazas-Velarde et al.[18–20] and Dernedde et al.[26,27] The CVMC used in the present work is based on the approach of Terrazas-Velarde et al.[19] The MC method is very useful for identifying the influencing parameters as it gives real microscale insight. Furthermore, many properties that are difficult to measure, such as moisture and structure of a particle, can easily be tracked down. Major drawbacks of MC methods include their stochastic nature and computational cost, which restricts their direct use in engineering applications.

Microscale Modeling

The MC method is a probabilistic approach to investigate a problem and by using the statistical properties of a finite sample of entities.[28–31] It can be thought of as a scaled-down virtual process. Once the simulation is complete, the results can be mapped to real findings by multiplying with a scale-up factor. The micromodel used in the present work is event driven CVMC and based on the work of Terrazas-Velarde et al.[19] to simulate the pure agglomeration process. Micro-processes such as collision of particles, deposition of droplets, drying of binder droplets, sticking, or rebound according to the Stokes criterion for the dissipation of kinetic energy, and so forth, are incorporated in the algorithm. A flow chart of the CVMC approach is given in Figure 2. The algorithm is briefly described in the following. For the detailed structure and operation of CVMC see Terrazas-Velarde et al.[19]

Brief description of the CVMC algorithm

The applied MC model is based on the collision events that take place between particles during SFBG and on the "concept of positions" on particle surface. The "concept of positions" used in the present study is taken from the work of Terrazas-Velarde et al.,[19] where it has been validated against experimental data. In this approach, the surface area of every particle is divided into sectors. The area of each sector is approximately set equal to the area blocked by a single primary particle on successful collision, that is, the number of sectors per primary particle determines the maximal coordination number of the primary particle. After a successful aggregation event, one sector from each involved particle is set as "blocked" and does not contribute further to the aggregation process. The other sectors of the particles are still accounted as available area that can be utilized for

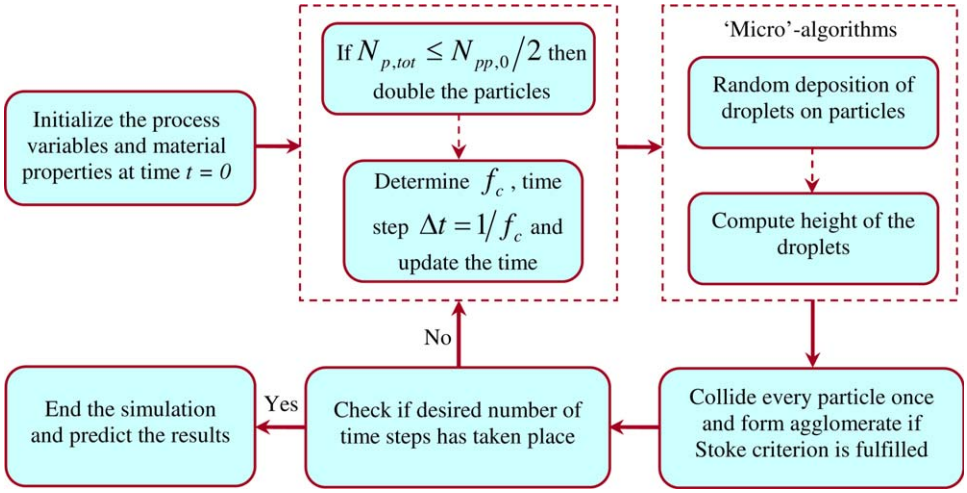

Figure 2. Schematic diagram of the CVMC algorithm used in the present work.

[Color figure can be viewed in the online issue, which is available at wileyonlinelibrary.com.]

droplet deposition and, hence, in agglomeration. This means that the shape of the particles is not necessarily taken as spherical in the microscale approach. Moreover, the area of each sector is further subdivided into smaller areas called positions. The area of each position is approximately set equal to the surface footprint of a droplet. This means, in a droplet deposition event, one position is set as completely "occupied or wet."

In the current CVMC model, we have taken the same process conditions and material properties as in Terrazas-Velarde et al.,[19] which means that the number of sectors per primary particle and the number of positions per primary particle have been calculated by using the sizes of droplets and primary particles of their experimental work (also given in Table 4). Under the conditions of Terrazas-Velarde et al.[19] and also in our work, a droplet's footprint area is calculated to be approximately 1/24th of the surface area of a primary particle. Moreover, during agglomeration of two primary particles, 8/24th of the total surface area (4/24th of the surface area of each primary particle involved) is considered to get blocked. This blockage of areas in an agglomeration event is called steric hindrance and assumed to be constant in the present study.

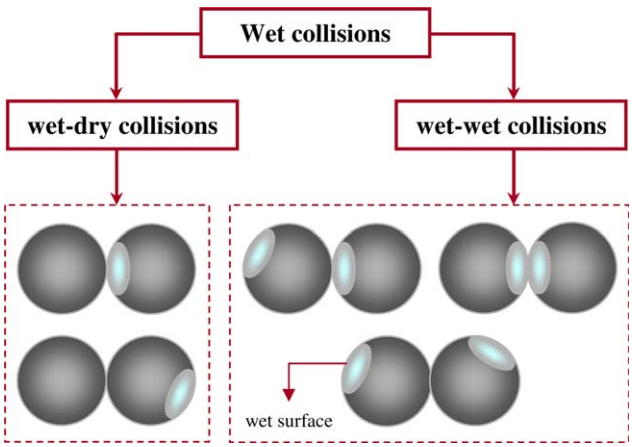

Figure 3. Wet collision scenarios.

[Color figure can be viewed in the online issue, which is available at wileyonlinelibrary.com.]

During each time step of MC, collisions between randomly chosen pairs of particles take place and a decision about successful or unsuccessful aggregation is made for each collision based on the following conditions:

1. check if the collision is a wet collision
2. check if particles strike at wet position/s
3. if particles strike at wet position/s, then check for coalescence/rebound condition by using the Stokes criterion developed by Ennis et al.[32]

If aforementioned conditions are satisfied then colliding particles form a new agglomerate. It is important to mention here that by wet collision we mean a collision in which a wet particle (either completely or partially wet) is involved. This implies that collision of wet particles at dry spot/s is also taken as a wet collision. Possible scenarios of wet collisions are shown in Figure 3.

Macroscale Modeling

The aim is to, first, identify the important influencing variables. This is achieved by observing the CVMC algorithm described in the previous section. Once such variables/parameters are identified, then they need to be incorporated in the kernel of the PBE and should be predicted independently. Furthermore, parameters with significant distribution at the microlevel, such as moisture distribution, need to be averaged for usage in the macro model. We start here by formulating an expression for the aggregation kernel, followed by modeling of variables/parameters involved.

Modeling the aggregation kernel

Equation 2 is the conventional form of an aggregation kernel, in which β_0 is usually fitted to data and some structure of $\beta^*(v, v')$ from literature is used based on flow patterns/motion. To correlate the process parameters with the kernel, we would first like to derive a mathematical expression for it by following Hussain et al.[17] It can be noticed that in the CVMC algorithm particles are selected randomly for binary collisions, that is, the process of selecting particles for collision does not take into account the sizes of the particles. Such a scenario is regarded in the population balance model

(PBM) as a size-independent aggregation process and $\beta^*(v, v')$ is taken to be unity, that is

$$\beta(t, v, v') = \beta_0(t)\beta^*(v, v') = \beta_0(t) \tag{3}$$

This means that aggregation kernel and aggregation efficiency are the same for our PBM, and we may use both terms interchangeably in the further discussion. The aggregation efficiency is commonly extracted from experimental results by the differential technique which uses the rate of change of the zeroth moment of the PSD.[1,33,34] The rate of change of the total number of particles, in case of size-independent kernel, is found to be

$$\left.\frac{dN_{\mathrm{p,tot}}(t)}{dt}\right|_{\mathrm{PBE}} = -\frac{\beta_0(t)N_{\mathrm{p,tot}}^2(t)}{2} \tag{4}$$

Moreover, the rate at which the particle number would change in MC depends on the total number of successful collisions. Thus in MC

$$\left.\frac{dN_{\mathrm{p,tot}}(t)}{dt}\right|_{\mathrm{MC}} = -\frac{f_s N_{\mathrm{p,tot}}(t)}{2} \tag{5}$$

where f_s is the frequency of successful collisions per particle. Comparing Eqs. 4 and 5 yields

$$\beta_0(t) = \frac{f_s}{N_{\mathrm{p,tot}}(t)} \tag{6}$$

Thus, the behavior of aggregation efficiency is merely dependent on the frequency of successful collisions per particle. The model for f_s can be formulated by observing the causes which make a collision successful in the MC. As mentioned earlier, a collision will be successful when the following three possibilities are fulfilled simultaneously.

1. Either Wet-Dry or Wet-Wet Collision Takes Place: The probability of selecting exactly one wet and one dry particle when two particles are randomly drawn from the total number of particles is

$$P_{\mathrm{c,wd}} = \frac{{}^{N_{\mathrm{p,wet}}}C_1 \times {}^{N_{\mathrm{p,dry}}}C_1}{{}^{N_{\mathrm{p,tot}}}C_2} = \frac{2N_{\mathrm{p,wet}}N_{\mathrm{p,dry}}}{N_{\mathrm{p,tot}}\left(N_{\mathrm{p,tot}}-1\right)} \tag{7}$$

Here, $P_{\mathrm{c,wd}}$ is the probability of wet-dry collision; C is the symbol for combination and $N_{\mathrm{p,dry}} = N_{\mathrm{p,tot}} - N_{\mathrm{p,wet}}$ represents the total number of dry particles. Similarly, the probability of selecting both particles wet when drawn randomly from the total number of particles is

$$P_{\mathrm{c,ww}} = \frac{{}^{N_{\mathrm{p,wet}}}C_2}{{}^{N_{\mathrm{p,tot}}}C_2} = \frac{N_{\mathrm{p,wet}}\left(N_{\mathrm{p,wet}}-1\right)}{N_{\mathrm{p,tot}}\left(N_{\mathrm{p,tot}}-1\right)} \tag{8}$$

Here, $P_{\mathrm{c,ww}}$ is the probability of wet-wet collision.

2. Particles Strike at Wet Position/s: This possibility is also divided into two parts, based on the occurrence of wet-dry or wet-wet collision. In the case of wet-dry collision, the chance that particles strike at wet surface η_{wd} is simply equal to the wet surface coverage fraction of the wet particle. In MC every wet particle may have a different wet surface coverage fraction which affects the collision at the microlevel. However, to introduce this effect at the macrolevel, we take an average value of wet surface coverage fraction per wet particle at time t, denoted by η. It follows that at different times, we have different average wet surface coverage fractions per wet particle. In the case of wet-wet collision, we neglect the possibility that wet positions of both wet particles hit each other, because of very low η. Then, the average probability that particles will strike at wet position in wet-wet collision can be computed by

$$\eta_{\mathrm{ww}} = \eta + \eta - 2\eta\eta = 2\left(\eta - \eta^2\right) \tag{9}$$

Here, η_{ww} represents the probability of having collision at wet position in a wet-wet collision case. The above expression for η_{ww} is computed by assigning an average size to all colliding particles at time t.

3. Kinetic Energy of the Colliding Particles is Dissipated by the Liquid Layer: In the MC, the Stokes criterion is used to compute whether the liquid layer will be able to dissipate the kinetic energy of the colliding particles or not. To include this effect in our model, we have used an average value of success fraction concerning the dissipation of kinetic energy, denoted by ψ. This average value is computed using the information extracted from the MC.

The possibilities 2 and 3 collectively can be regarded as the adhesion probability (P_{adhes}) of the colliding particles

$$P_{\mathrm{adhes,wd}} = \eta_{\mathrm{wd}}\psi = \eta\psi, P_{\mathrm{adhes,ww}} = \eta_{\mathrm{ww}}\psi = 2\psi\left(\eta - \eta^2\right) \tag{10}$$

Here, $P_{\mathrm{adhes,wd}}$ and $P_{\mathrm{adhes,ww}}$ are adhesion probabilities for wet-dry and wet-wet collisions, respectively. A collision event turns into an aggregation event when all three possibilities (1, 2, and 3) take place simultaneously. If f_c is the collision frequency, that is, the number of collisions per second per particle, then the frequency of successful collisions f_s can be modeled by multiplying the wet collision probability $P_{\mathrm{c,wet}}$ with the adhesion probability P_{adhes} as

$$f_s = f_c\left(P_{\mathrm{adhes,wd}} \times P_{\mathrm{c,wd}} + P_{\mathrm{adhes,ww}} \times P_{\mathrm{c,ww}}\right) \tag{11}$$

Hence, using Eqs. 7, 8, and 10 in 11 we obtain

$$f_s = f_c\psi\frac{N_{\mathrm{p,wet}}}{N_{\mathrm{p,tot}}}\left(\frac{2\left(N_{\mathrm{p,tot}} - N_{\mathrm{p,wet}}\right)}{N_{\mathrm{p,tot}}-1}\eta_{\mathrm{wd}} + \frac{N_{\mathrm{p,wet}}-1}{N_{\mathrm{p,tot}}-1}\eta_{\mathrm{ww}}\right) \tag{12}$$

Substituting Eq. 12 in Eq. 6 gives the expression for the aggregation kernel (efficiency) that should be used in PBE to compare its results (e.g., PSD) with the MC

$$\beta = \beta_0 = f_c\psi\frac{N_{\mathrm{p,wet}}}{N_{\mathrm{p,tot}}^2}\left(\frac{2\left(N_{\mathrm{p,tot}} - N_{\mathrm{p,wet}}\right)}{N_{\mathrm{p,tot}}-1}\eta_{\mathrm{wd}} + \frac{N_{\mathrm{p,wet}}-1}{N_{\mathrm{p,tot}}-1}\eta_{\mathrm{ww}}\right) \tag{13}$$

Modeling the variables affecting β_0

Equation 13 can not be used in Eq. 1 unless we have the information about $f_c, N_{\mathrm{p,tot}}, N_{\mathrm{p,wet}}, \eta$, and ψ prior to the simulation or during the simulation. It should be noted that the value ψ is taken to be constant and extracted from the MC for its usage in the model. The modeling of ψ will be addressed in a separate article, because we are continuing our efforts in that direction. The focus here is to predict $N_{\mathrm{p,tot}}, N_{\mathrm{p,wet}}$, and η, the time-dependent factors of $\beta_0(t)$. The average wet surface coverage fraction per wet particle η is directly correlated to the number of droplets (N_{drop}) in the system. Thus, N_{drop} needs to be modeled to predict η.

Equation for $N_{\mathrm{p,tot}}$

The total number of particles can easily be modeled using Eq. 13 in Eq. 4

$$\frac{dN_{p,tot}}{dt} = -\frac{f_c \psi N_{p,wet}}{2}\left(\frac{2\left(N_{p,tot} - N_{p,wet}\right)}{N_{p,tot} - 1}\eta_{wd} + \frac{N_{p,wet} - 1}{N_{p,tot} - 1}\eta_{ww}\right) \tag{14}$$

Equation for $N_{p,wet}$

The total number of wet particles (particles with accessible wet surface) in the system at any time t can be modeled by observing the factors responsible for their births and deaths in the MC. From the MC, it can easily be found that the birth of wet particles is directly influenced by the rate at which binder liquid droplets enter the granulator. Moreover, the death rate of wet particles is dependent on two main factors: (1) death of wet particles due to aggregation and (2) deposited droplets on the particles get dry convectively due to the hot air passing through the granulator. As we consider only nonporous particles at this stage, we neglect the effect that simultaneous penetration of liquid in a porous primary particle ("imbibition") may have on sessile droplet drying. The rate at which wet particles get dry due to aggregation can further be subdivided into two parts, based on the wet-dry and wet-wet collision cases. Thus, a generalized equation for the total number of wet particles in the SFBG at any time t can be written as

$$\frac{dN_{p,wet}}{dt} = B_{p,wet} - D^{agg}_{p,wet,wd} - D^{agg}_{p,wet,ww} - D^{dryng}_{p,wet} \tag{15}$$

Here, $B_{p,wet}$ is the birth rate of wet particles, $D^{agg}_{p,wet,wd}$ denotes the rate at which wet particles will get dry due to the aggregation of wet-dry particles, $D^{agg}_{p,wet,ww}$ is the rate of death of wet particles due to aggregation of wet-wet particles, and $D^{dryng}_{p,wet}$ represents the rate of convective drying of wet particles. The birth rate of wet particles is directly connected to the rate at which droplets are deposited on the particles, that is, $\dot{N}^{in}_{drop}$, wherein the superscript "in" denotes "influx of droplets." However, all droplets entering in the system do not play role in the birth of wet particles. There can be many droplets which may get deposited on already wet particles. Therefore, the birth rate of wet particles is computed by subtracting the number of wet particles chosen for droplet deposition from the droplet addition rate

$$B_{p,wet} = \dot{N}^{in}_{drop} - \dot{N}^{in}_{drop}\left(\frac{N_{p,wet}}{N_{p,tot}}\right) = \dot{N}^{in}_{drop}\left(1 - \frac{N_{p,wet}}{N_{p,tot}}\right) \tag{16}$$

The death rate of wet particles due to aggregation can be modeled by considering the death rates due to wet-dry and wet-wet aggregation separately. We consider loss of one droplet in every successful collision, except when wet positions of both wet particles hit each other and form an agglomerate. The later case results in loss of two droplets. It is important to mention here that a new agglomerate is considered as completely dry only when formed by consuming all moisture during a wet collision. This means that when a wet particle has only one droplet deposited on it, then one wet particle is taken to be lost in aggregation due to wet-dry collision. Similarly, two wet particles should be considered as dead when an agglomerate is formed by contact of a wet surface with another wet surface in a wet-wet collision; (This case is neglected as it will be discussed later in this section). Such possibilities are available at the initial stage of the agglomeration process, when the concentration of wet particles is not high. However, with the passage of time more particles become wet, and the probability of a droplet deposition on a wet particle increases. Under these circumstances, a successful aggregation event may not contribute to the loss of a wet particle. For instance, when a dry particle collides with a wet particle having more than one droplet, then successful collision would still result in a wet granule. The possible results of wet collision at wet spots are summarized in Figure 4.

The death rate of wet particles due to the aggregation of wet-dry particles can be computed by finding the total number of wet-dry collisions and multiplying the result with the adhesion probability. The total number of collisions denoted by $\dot{N}_{c,tot}$ at time t is given by

$$\dot{N}_{c,tot} = \frac{N_{p,tot} f_c}{2} \tag{17}$$

Multiplication of Eq. 17 and Eq. 7 yields the total number of wet-dry collisions in unit time

$$\begin{aligned}\dot{N}_{c,wd} &= \frac{f_c N_{p,tot}}{2}\left(\frac{2N_{p,wet}\left(N_{p,tot} - N_{p,wet}\right)}{N_{p,tot}\left(N_{p,tot} - 1\right)}\right) \\ &= \frac{f_c N_{p,wet}\left(N_{p,tot} - N_{p,wet}\right)}{\left(N_{p,tot} - 1\right)}\end{aligned} \tag{18}$$

where $\dot{N}_{c,wd}$ denotes the rate of wet-dry collisions. Finally, Eq. 18 should be multiplied by the ratio of wet particles to droplet number and with the adhesion probability for wet-dry collision (Eq. 10) to model the death rate of wet particles due to wet-dry aggregation. The ratio of $N_{p,wet}$ to N_{drop} is used as a multiplier to compute the fraction of wet particles lost in every successful wet-dry collision. The death term due to aggregation of wet-dry particles then takes the form

$$D^{agg}_{p,wet,wd} = f_c \eta_{wd} \psi \frac{N^2_{p,wet}}{N_{drop}}\left(1 - \frac{N_{p,wet} - 1}{N_{p,tot} - 1}\right) \tag{19}$$

The death rate of wet particles due to aggregation of wet-wet particles, as discussed earlier, can further be subdivided into two parts, depending on the contact point of the particles. The collision of a wet position of one particle with the wet position of the other particle consumes two droplets and is expected to be very less probable, especially when droplet size is taken to be very small with respect to the size of the primary particles, which is usually the case in SFBG. Thus, we simplify our model by ignoring such collisions. This simplification results in the death of one wet particle in a successful wet-wet collision, same as in the case of wet-dry collision. Then, the rate at which wet particles get dry due to the aggregation of wet-wet particles is computed by calculating the number of wet particles involved in the wet-wet collision and multiplying it by the adhesion probability. The total number of wet-wet collisions in unit time $\left(\dot{N}_{c,ww}\right)$ can be found by taking the product of Eqs. 17 and 8 as

$$\dot{N}_{c,ww} = \frac{f_c N_{p,tot}}{2}\left(\frac{N_{p,wet}\left(N_{p,wet} - 1\right)}{N_{p,tot}\left(N_{p,tot} - 1\right)}\right) = \frac{f_c N_{p,wet}\left(N_{p,wet} - 1\right)}{2\left(N_{p,tot} - 1\right)} \tag{20}$$

Note that, we did not multiply Eq. 20 by 2 because each successful wet-wet collision consumes only one wet particle due to the simplification taken into account. The death of wet particles due to aggregation of wet-wet particles is then modeled by multiplying Eq. 20 with the adhesion probability for wet-wet collision, resulting in

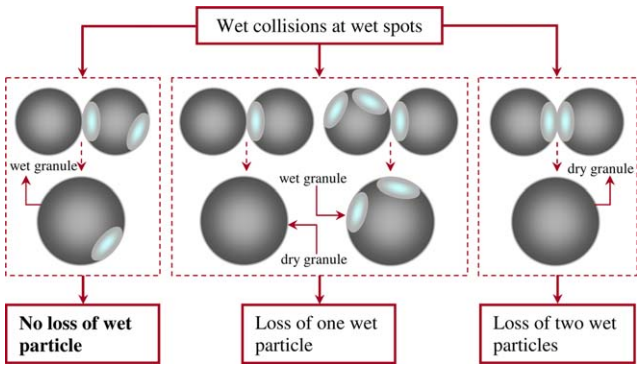

Figure 4. Possible results of wet collisions at wet spots.

[Color figure can be viewed in the online issue, which is available at wileyonlinelibrary.com.]

$$D^{\text{agg}}_{\text{p,wet,ww}} = \frac{1}{2} f_c \eta_{\text{ww}} \psi N_{\text{p,wet}} \left(\frac{N_{\text{p,wet}} - 1}{N_{\text{p,tot}} - 1} \right) \tag{21}$$

The final step in modeling the death rate term of wet particles is modeling the death rate of wet particles due to drying of the droplets, which may be written as

$$D^{\text{dryng}}_{\text{p,wet}} = \frac{\tilde{N}_{\text{p,wet}}}{\tau} \frac{N_{\text{p,wet}}}{N_{\text{drop}}} \tag{22}$$

where τ is the convective drying time of a droplet. $\tilde{N}_{\text{p,wet}}$ is the reduced number of wet particles that should be considered for drying. It is further multiplied by $N_{\text{p,wet}}/N_{\text{drop}}$ to dry the correct number of wet particles if wet particles contain more than one droplet. The reduced number of wet particles is required to approximate the effect of aggregation on drying of accessible droplets. This can be explained by an example. Assume that a droplet is deposited on a particle at time t_a which means that this droplet could "stay alive" until the time $t_b = t_a + \tau$ has been reached. However, during the time period τ, the droplet may still get consumed in aggregation and become inaccessible. Hence, the concentration of accessible droplets and, consequently, the concentration of wet particles decreases due to aggregation. To compute the reduced number of wet particles, we consider the death rate of wet particles due to aggregation (Eqs. 19 and 21) and write an ordinary differential equation for $\tilde{N}_{\text{p,wet}}$ as

$$\frac{d\tilde{N}_{\text{p,wet}}(\tilde{t},t)}{dt} = -\frac{\psi f_c \eta_{\text{wd}} \tilde{N}_{\text{p,wet}}}{2} \left(\frac{N_{\text{p,wet}}}{N_{\text{drop}}} - \left(\frac{N_{\text{p,wet}}}{N_{\text{drop}}} - \frac{\eta_{\text{ww}}}{2\eta_{\text{wd}}} \right) \frac{\tilde{N}_{\text{p,wet}} - 1}{N_{\text{p,tot}} - 1} \right); \tilde{N}_{\text{wet}}(0,t) = N_{\text{wet}}(t). \tag{23}$$

Here, $\tilde{t}$ is the time over which Eq. 23 is to be integrated in the interval $[0, \tau]$ at process time t. The wet particles consumed due to aggregation during the time period τ may get wet again due to droplet deposition. This effect of simultaneous wetting and drying has been approximated by using a factor of $1/2$ on the right-hand side of Eq. 23. We have assumed in modeling of Eq. 23 that τ is less than the process time. The aforementioned approach has been extensively checked for several combinations of f_c and τ and found to be accurate.

Figure 5 provides a comparison of the number of wet particles predicted with and without the effect of aggregation on drying. Results shown in Figure 5 are generated with the process conditions of Set-A simulations (see Tables 2 and 3). All other necessary parameters have been extracted from the MC. It can be seen that by incorporating the effect of aggregation on convective drying results in a slightly better match with the number of wet particles from the MC.

The model for prediction of wet particles can then be finally formulated by using Eqs. 16, 19, 21, and 22 in Eq. 15

$$\frac{dN_{\text{p,wet}}}{dt} = \dot{N}^{\text{in}}_{\text{drop}} \left(1 - \frac{N_{\text{p,wet}}}{N_{\text{p,tot}}} \right) - f_c \eta_{\text{wd}} \psi N_{\text{p,wet}} \left(\frac{N_{\text{p,wet}}}{N_{\text{drop}}} - \left(\frac{N_{\text{p,wet}}}{N_{\text{drop}}} - \frac{\eta_{\text{ww}}}{2\eta_{\text{wd}}} \right) \left(\frac{N_{\text{p,wet}} - 1}{N_{\text{p,tot}} - 1} \right) \right) - \frac{\tilde{N}_{\text{p,wet}}}{\tau} \frac{N_{\text{p,wet}}}{N_{\text{drop}}} \tag{24}$$

Equation for N_{drop}

The total number of droplets in the granulator is modeled in the same way as the number of wet particles. Similar to the MC, we assume here that a droplet can not be deposited onto another deposited droplet. This means that every droplet deposition affects the wet surface coverage fraction. The birth rate B_{drop} for N_{drop} is then

$$B_{\text{drop}} = \dot{N}^{\text{in}}_{\text{drop}} \tag{25}$$

Equation 22, which serves here as the death rate of droplets due to convective drying, is updated by replacing the factor $N_{\text{p,wet}}/N_{\text{drop}}$ with $N_{\text{drop}}/N_{\text{p,wet}}$. This would provide us the total number of droplets to be dried when multiplied with $\tilde{N}_{\text{p,wet}}$. Furthermore, the death rate of droplets due to aggregation is computed by multiplying the death rate of wet particles due to aggregation by $N_{\text{drop}}/N_{\text{p,wet}}$. However, we assume that every aggregation event, even if the resulting granule remains wet, consumes one droplet. Hence, we do not consider the factor $N_{\text{p,wet}}/N_{\text{drop}}$ in Eq. 19 to model the death rate of droplets due to wet-dry aggregation. Considering these facts, Eq. 24 is modified to predict N_{drop} as

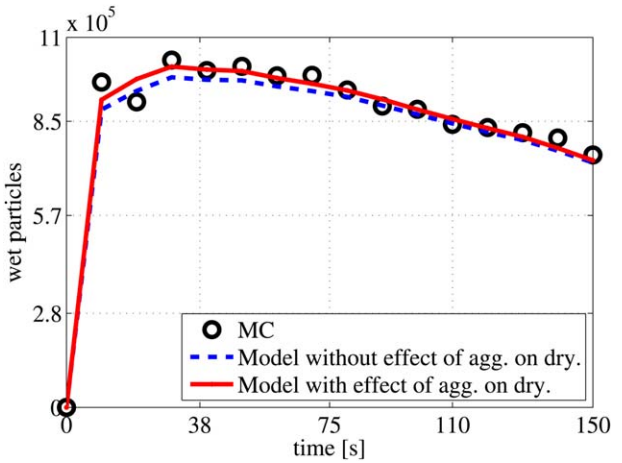

Figure 5. Comparison of $N_{\text{p,wet}}$ computed with and without effect of aggregation on drying.

[Color figure can be viewed in the online issue, which is available at wileyonlinelibrary.com.]

$$\frac{dN_{\text{drop}}}{dt} = \dot{N}_{\text{drop}}^{\text{in}} - N_{\text{drop}} \left(f_c \eta_{\text{wd}} \psi \left(1 - \left(1 - \frac{\eta_{\text{ww}}}{2\eta_{\text{wd}}} \right) \left(\frac{N_{\text{p,wet}} - 1}{N_{\text{p,tot}} - 1} \right) \right) + \frac{\tilde{N}_{\text{p,wet}}}{\tau N_{\text{p,wet}}} \right) \tag{26}$$

The average wet surface coverage fraction per wet particle η is computed during the PBM simulation by

$$\eta = \frac{N_{\text{drop}} \eta_{\text{pp}}}{N_{\text{p,wet}} A} \tag{27}$$

Here, η_{pp} is the surface coverage fraction of one droplet on a primary particle and is taken to be $A_{\text{pp}}/24$, where A_{pp} is the primary particle surface area. In Eq. 27, A is the mean surface area of the particles at time t. We know that each aggregation event decreases the surface area of colliding particles by two sectors, hence A is calculated as

$$A = \frac{A_{\text{pp}}}{6N_{\text{p,tot}}} \sum_{i=1}^{m} ((4i+2)N_i) \tag{28}$$

where m is the number of primary particles in the largest agglomerate and N_i is the number of agglomerates with i primary particles at time t.

Final remarks

Evaluation of N_{drop} completes the development of our PBM. The system of Eqs. 1, 13, 14, 24, and 26 forms a comprehensive PBM that takes into account the process conditions during simulation. For better understanding, assumptions taken into account in modeling of the PBM are summarized in Table 1.

To solve the PBM, we still need information about three more parameters, namely collision frequency per particle f_c, average success fraction concerning the dissipation of kinetic energy ψ, and the drying time τ of a droplet. The average values of f_c and ψ are extracted from the MC simulations. The vector containing the values of f_c at each time step is extracted from the MC and then a mean value of f_c is calculated. The effect of dissipation of kinetic energy during any binary collision is included in the PBM by computing an average value of the success ratio from the Stokes criterion in the MC. Success ratios according to Stokes criterion are computed in each time step of the MC by dividing the number of times the Stokes criterion is fulfilled with the number of times particles have collided at wet position/s. These values are then further averaged to capture the overall effect of dissipation of kinetic energy. It should be noted that the values of f_c and ψ are used in the simulation prior to the simulation, that is, it is not the case that these values are chosen in a way that the results of PBM show a good match with MC. Moreover, both constant values appear in front of Eq. 13 as product of each other which serves as a scaling factor.

Results and Discussion

The developed model (Eqs. 1, 13, 14, 24, and 26) has been validated by comparing the results with CVMC simulations. For this purpose, two sets of MC and PBM simulations with variation of two operating parameters, namely binder liquid mass flow rate $\dot{M}_l$ and initial binder mass fraction x_b are discussed here. Further sets of simulations conducted by varying other operating parameters, such as gas inlet temperature, behave in a similar way. The sets of simulations to be presented are denoted by Set-A and Set-B, and are further subdivided into MC and PBM simulations, as shown in Table 2.

Table 1. Assumptions of the PBM

1	Collisions are size independent
2	Steric hindrance remains constant during agglomeration process
3	A droplet can not be deposited on a wet position
4	Only accessible droplets are considered for drying
5	Collisions at wet spots of two wet particles are neglected

Table 2. Denotation of Simulations with Varied Parameters

Set-A (Binder Addition Rate)		Set-B (Binder Mass Fraction)	
MC-01	PBM-01	MC-01	PBM-01
MC-02	PBM-02	MC-04	PBM-04
MC-03	PBM-03	MC-05	PBM-05

Set-A corresponds to simulations performed with variation in binder mass flow rate, whereas Set-B represents simulations carried out with variation in initial binder mass fraction. Each set contains three MC and three PBM simulations with a unique value of binder mass flow rate or initial binder mass fraction, whereas all other process conditions and material properties remain the same. All simulations represent a batch mode of lab-scale agglomeration experiments in which the gas mass flow rate stays constant. The description of the different simulations and varied parameters is summarized in Table 3.

The other process conditions and material properties required to run the simulations are summarized in Table 4. To validate the PBM, results are generated from the CVMC with the process conditions and material properties as described in Tables 3 and 4 for all sets of MC "experiments." In the second step, results from PBM are produced by simultaneous numerical solution of the system of Eqs. 1, 13, 14, 24, and 26. All process conditions and material properties are kept the same as in Tables 3 and 4. The values of f_c, ψ, and τ are illustrated in Table 5.

By observing Table 5, it can be concluded that the average collision frequency per particle more or less remains the same for all simulations. The empirical correlation that has been used in MC[19] to calculate f_c depends on two factors: gas fluidization velocity and volume of expanded bed. As the gas fluidization velocity remains the same and constant for all simulations, the only factor responsible for any change in the average value of f_c is the volume of expanded bed. Therefore, the small variations in the values of f_c could be explained by the fact that with the passage of time the volume of the bed decreases due to increasing size, and, hence weight of particles. Consequently, the value of f_c is expected to be slightly lower in the case of higher aggregation rate. This can be observed from Table 5 and results of

Table 3. Simulations with the Corresponding Values of the Varied Parameters

Simulations	Binder Mass Flow Rate (g/h)	Binder Mass Fraction (wt %)
MC-01, PBM-01	300	8
MC-02, PBM-02	100	8
MC-03, PBM-03	500	8
MC-04, PBM-04	300	4
MC-05, PBM-05	300	10

Table 4. Process Conditions and Material Properties

Parameter	Symbol	Quantity	Unit
Bed mass	M_{bed}	500	g
Primary particle diameter	d_{pp}	0.4	mm
Particle density	ρ_p	2400	kg/m^3
Particle surface asperities height	h_a	0.01	mm
Particle restitution coefficient	e	0.8	–
Droplet diameter	d_{drop}	80	μm
Particle-droplet contact angle	θ	40	degree
Binder mass fraction	x_b	4–10	wt %
Binder liquid density	ρ_l	1020	kg/m^3
Binder volumetric flow rate	$\dot{V}_l$	100–500	ml/h
Collision velocity, mean value	u_c	0.675	m/s
Fluidization velocity	u_g	1.35	m/s
Gas mass flow rate	$\dot{M}_g$	100	kg/h
Gas inlet temperature	T_g	30	^{o}C
Molar fraction of vapor in the gas	$\tilde{y}_g$	0.0023–0.0086	–
Moisture content in the gas	Y_g	1.4–5.4	g/kg
Initial number of primary particles in MC simulation box	$N_{pp,MC,0}$	2000	–

sections Variation of Binder Mass Flow Rate and Variation of Binder Mass Fraction.

As mentioned earlier, ψ represents an average value of the success fraction regarding the dissipation of kinetic energy for collisions at wet spots. For instance, in PBM-01 $\psi=0.67$signifies that 67% of all collisions that have taken place on wet spots were successful in the course of the simulation. During the early stage of the agglomeration process, it is expected that the kinetic energy will be dissipated in almost every collision at a wet spot, due to small particle size. Therefore, ψ is close to unity at this time. However, with the passage of time the average size of particles increases and the chance to fulfill the Stokes criterion decreases. Therefore, ψ also decreases. It can be observed from Table 5 that ψ has almost the same value for all simulations except for PBM-04. Here, ψ shows a significant decrease in its value as compared to the other simulations. This is due to low binder mass fraction (4%). With such a low binder mass fraction, one can expect rebounds in many wet collisions, especially with growing mean size of particles. Therefore, the value of ψ drops down significantly in this case.

The values of τ shown in Table 5 have been calculated by using the model given in Terrazas-Velarde et al.[19] According to this model, the drying time is inversely proportional to the difference in vapor pressure between particle surface and the bulk of the gas. Water vapor pressure at the particle surface is calculated at adiabatic saturation temperature. The bulk of the gas is assumed to be perfectly backmixed in the model, so that vapor pressure, molar fraction $\tilde{y}_g$ and moisture content Y_g in this bulk (cf. Table 4) increase with increasing mass flow rate of binder liquid. Therefore, the driving force for drying decreases and the drying time τ increases from PBM-02 to PBM-01 and PBM-03 in Table 5. On the contrary, the simple drying model by Terrazas-Velarde et al.[19] does not account for any influence of binder mass fraction under the same conditions on drying time. Consequently, the same drying time is used for PBM-01, PBM-04, and PBM-05 in Table 5.

Variation of binder mass flow rate

The results generated in Set-A simulations (variation of binder mass addition rate) are plotted in Figures 6, 8, and 9. All figures show a good match of MC and PBM results. It is expected that with the increase of binder addition rate the aggregation rate increases, because of increase in the concentration of wet particles, which means that the chance of wet collisions increases and, hence, the probability of a collision to be successful also increases. This further implies that the aggregation efficiency increases with an increase in binder addition rate, a behavior that can easily be observed in Figures 6 and 8.

All simulations were run for 200 s except MC-03 which is plotted for a process time of 140 s. The reason is that MC-03 and, hence, PBE-03 have very high binder mass flow rate due to which particles get aggregated very rapidly. This can be observed in Figure 6a that provides a comparison of normalized total number of particles predicted in MC and PBM. It can be seen that in MC-03 and PBM-03, a degree of aggregation of around 95% has been achieved in 140 s, whereas at the same time simulations with binder mass flow rates of 100 and 300 g/h show around 60 and 80% degree of aggregation, respectively.

Furthermore, due to high binder mass flow rate in MC-03 almost all particles become wet after a certain time, as can be seen in Figure 7. Due to high binder flow rate, the concentration of droplets increases rapidly to a high value that can be observed in Figure 6c. Therefore, a relatively large number of wet collisions takes place and the aggregation rate increases. PBM takes all these facts into account and predicts the results accordingly. The number of wet particles (Figure 6d) predicted by PBM also gives a very good match with the number of wet particles from MC. Furthermore, the wet surface coverage fraction per wet particle (η) computed using Eq. 29 also provides a good approximation to the results of MC (Figure 6b). The wet surface coverage fraction per wet particle decreases with time because of two reasons: (1) total surface area of wet particles increases with time and (2) the concentration of droplets is affected by consumption of droplets in agglomeration and convective drying of droplets. This means, the number of droplets present on the surfaces of particles at any time is less than the total influx of droplets in the system. Furthermore, the total surface area of wet particles increases with time due to aggregation, which also plays role in decreasing the average wet surface coverage fraction per wet particle. We can expect an increase in η when all particles become wet. This can be observed in the case of mass flow rate of 500 g/h in Figure 6b. It is shown further in Figure 7 that in this case more or less all particles in the system became wet after 110 s.

The comparison between predicted and extracted aggregation efficiencies is demonstrated in Figure 8. The results shown in Figure 8 are encouraging and prove that the developed aggregation kinetic model (Eq. 13) is capable of

Table 5. Values of f_c,ψ, and τ

Sim. # Params.	PBM-01	PBM-02	PBM-03	PBM-04	PBM-05
$f_c(s^{-1})$	1.85	1.86	1.80	1.88	1.84
$\psi(-)$	0.67	0.69	0.70	0.58	0.69
τ(s)	3.8	3.3	4.2	3.8	3.8

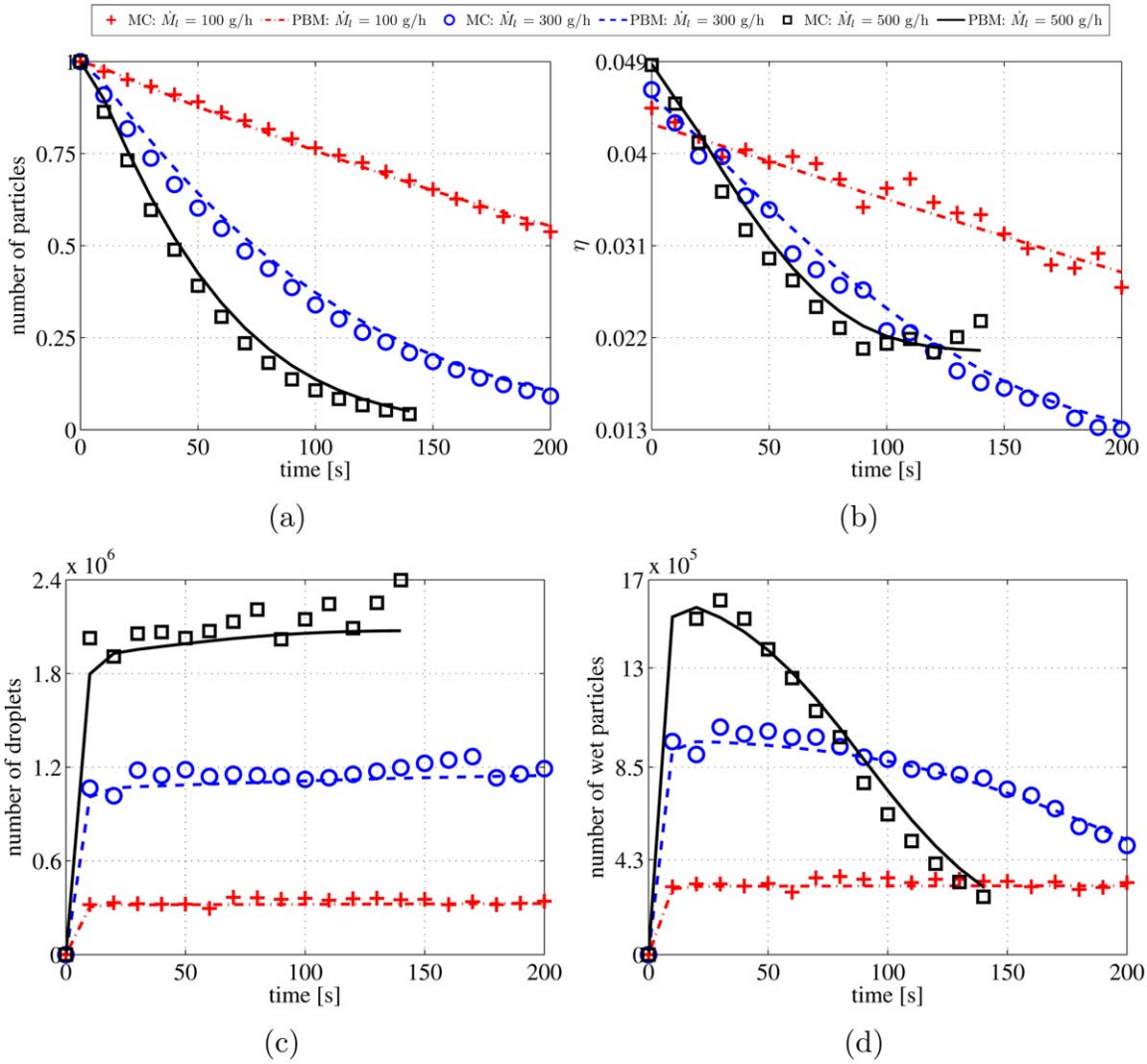

Figure 6. Comparison of MC and PBM results for Set-A simulations: (a) Normalized total number of particles, (b) wet surface coverage fraction per wet particle, (c) number of droplets, (d) number of wet particles; Results for MC-03 and PBM-03 have been plotted until 140 s.

[Color figure can be viewed in the online issue, which is available at wileyonlinelibrary.com.]

capturing the effect of binder mass flow rate on the aggregation process with good accuracy.

All results shown in Figures 6 and 8 would, though, not make sense if the final PSD could not be predicted with acceptable accuracy by the PBM. Hence, the PSDs at final times are presented separately in Figure 9 for the simulations of Set-A at three different binder mass flow rates. All plots show a good agreement between MC data and PBM predictions. In Figure 9 and all other figures where PSDs have been plotted (Figure 12), the particle sizes have been described by the number of primary particles they contain. In such figures, the abscissa represents the number of primary particles per agglomerate, whereas the ordinate shows the number of particles/agglomerates. For instance, Figure 9c shows that at 140 s, we have in the system 1.03×10^4 agglomerates composed of one primary particle, 9.93×10^3 agglomerates composed of two primary particles, 9.52×10^3agglomerates composed of three primary particles, and so on. The shape of the PSD is expected to be exponential like, as shown in Figures 9 and 12. This is because of two reasons: (1) the initial PSD is taken to be mono dispersed and (2) no effect of flow pattern is included in our model (also in MC), that is, the size-dependent part of the aggregation kernel is taken to be unity. It is also important to mention here that the proposed PBM is significantly computational efficient as compare to the MC. For instance, PBM-01 takes 11 s, whereas MC-01 requires approximately 2 h, to run the simulation of 200 s on a computer with i5–750 processor with 2.67 GHz of clock speed.

Variation of binder mass fraction

In Set-B of simulations, the initial binder mass fraction of droplets (x_b) is varied from 4 to 10%, as described in Table 3. The comparison of results of MC and PBM simulations is presented for the normalized number of particles, the wet surface coverage fraction per wet particle, the total number of droplets, the total number of wet particles, the aggregation efficiency, and the PSD in Figures 10–12.

Increasing the binder mass fraction in the droplet increases the viscosity of the binder and the capability of the liquid layer on the particle to dissipate the kinetic energy of the binary collision, so that we can expect higher aggregation

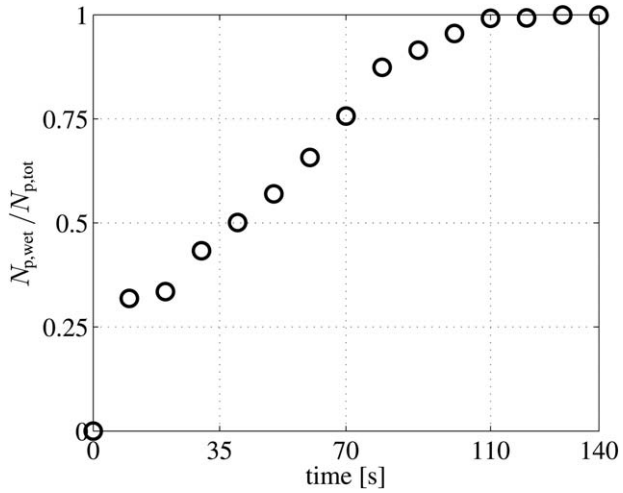

Figure 7. Ratio of wet particles to total particles for MC-03 simulation: due to high binder addition rate, all particles get wet after 110 s.

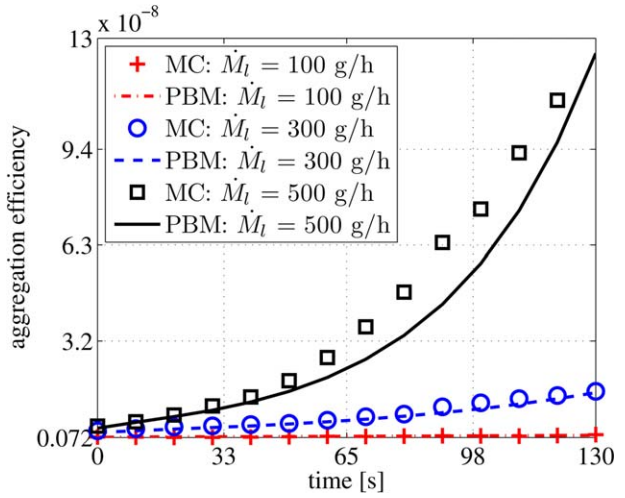

Figure 8. Aggregation efficiencies (β_0) computed from Eq. 13 are compared against extracted aggregation efficiencies for simulations of Set-A.

[Color figure can be viewed in the online issue, which is available at wileyonlinelibrary.com.]

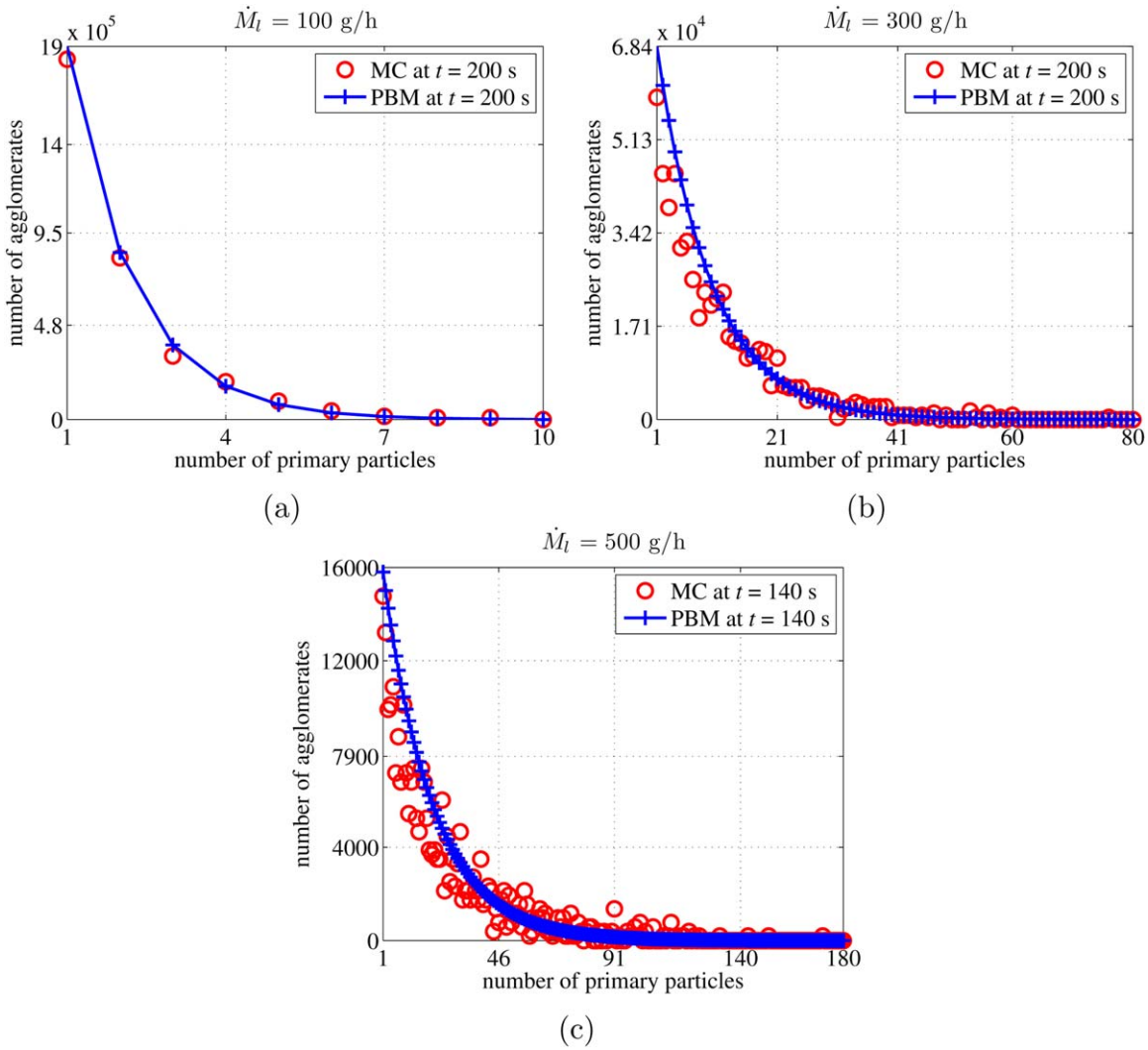

Figure 9. PSDs predicted from simulations of Set-A at $t = 200$ s: (a) MC-01, PBM-01; (b) MC-02, PBM-02; at $t = 140$ s: (c) MC-03, PBM-03.

[Color figure can be viewed in the online issue, which is available at wileyonlinelibrary.com.]

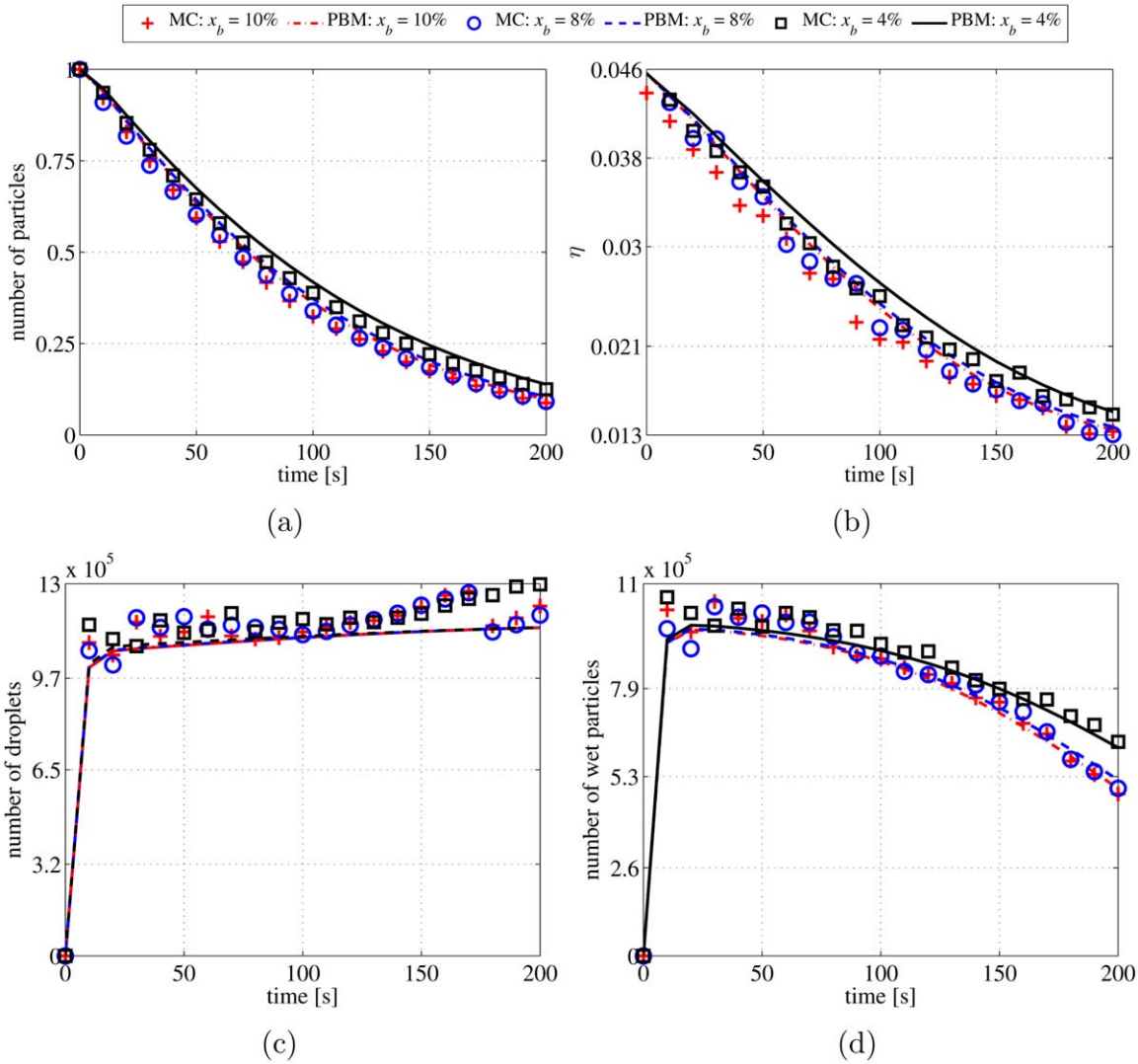

Figure 10. Comparison of MC and PBM results for Set-B simulations: (a) Normalized total number of particles, (b) wet surface coverage fraction per wet particle, (c) number of droplets, and (d) number of wet particles.

[Color figure can be viewed in the online issue, which is available at wileyonlinelibrary.com.]

efficiency and, hence, higher aggregation rate. This effect can be observed in Figures 10a and 11 but it is not very strong, because all other process conditions were the same in these simulations, resulting in more or less the same values of f_c, τ, and ψ for all simulations of Set-B (Table 5). An exception is the relatively small value of ψ for MC-04 and PBM-04, which is expected because of very low binder mass fraction in this case.

Results of simulations with the two highest binder mass fractions (MC-05 and MC-01) are very close to each other, because process conditions are otherwise the same and the difference in binder mass fraction between MC-01 and MC-05 is only 2%. Simulation results with the smallest binder mass fraction (x_b=4%) although show higher number of wet particles (Figure 10d) and the smallest aggregation rate (Figure 10a), with significant difference from the other simulations. Droplets with only 4% of binder mass fraction have a relatively small chance of fulfilling the Stokes criterion with increasing average size of particles. Therefore, we can expect relatively low aggregation rate in this case (Figure 11). Wet surface coverage fraction per wet particle (Figure 10b) behaves similar as the number of particles (Figure 10a), whereas the number of droplets (Figure 10c) remains essentially constant with changing binder mass fraction. In all these cases, the developed PBM demonstrates its strength by predicting the results of the MC with high accuracy and in an efficient way.

The computed aggregation efficiencies from Eq. 13 for all population balance simulations of Set-B are compared with aggregation efficiencies extracted from the corresponding MC simulations in Figure 11. The highest and lowest aggregation efficiencies are shown by MC-05 with x_b=10% and MC-04 with x_b=4%, respectively. It can be observed easily from Figure 11 that the predictions of the model (Eq. 13) match precisely with the MC results. The behavior of β_0 with changing binder mass fraction is captured by the model satisfactorily, which reveals its potential despite of conducted simplifications.

As mentioned earlier, the agreement of PSDs computed by the PBM comprising of Eqs. 1, 20, 21, 22, and 23 with PSD's resulting from the MC approach is of crucial importance. Figure 12 demonstrates this agreement for Set-B simulations. The PSD's of MC-01 and PBE-01 are

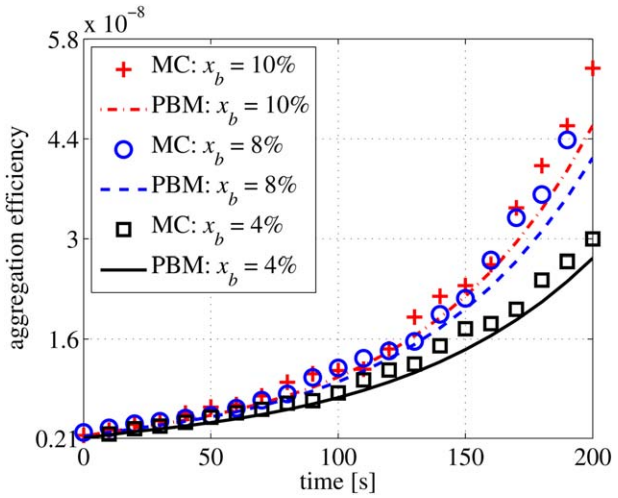

Figure 11. Comparison of aggregation efficiencies (β_0) computed from Eq. 13 with aggregation efficiencies extracted from MC simulations for different binder mass fractions.

[Color figure can be viewed in the online issue, which is available at wileyonlinelibrary.com.]

not compared in Figure 12, as this has already done in Figure 6a.

Remarks

After having discussed the results of the proposed model in a realistic window of operating conditions, we would like to briefly comment on its viability for practical applications. In addition to the process conditions, one needs to know f_c, τ, and ψ in advance to apply the PBM to simulate SFBG. The drying time τ can be calculated separately from a more or less sophisticated model for the drying of sessile droplets as, for example, from the model presented in Terrazas-Velarde et al.[19] Concerning f_c, Terrazas-Velarde et al.[19] have shown that the influence of operating parameters on the collision frequency can be predicted from the literature correlations, but absolute values need to be adapted. This is done by comparing MC results with the results of one SFBG experiment to fit the prefactor of literature correlation for f_c to a constant value. Regarding the overall success fraction concerning the dissipation of kinetic energy, ψ, it can be obtained from a few MC data, as done in the present work. However, derivation from MC constitutes a certain limitation, and it would be better to model this parameter within the PBM frame. Such modeling of the overall success fraction ψ is a challenging problem and subject of ongoing work. The aim is to develop an independent PBM with as few as possible fitting parameters to simulate spray fluidized bed agglomeration at the macroscale.

Conclusions

The effect of micro-processes on the macroscopic behavior of SFBG has been investigated. In this frame, the simulation of SFBG by means of population balances is supported and developed by studying the micro–macro interactions in MC simulations. A microscale approach based on CVMC simulations of Terrazas-Velarde et al.[19] was used to analyze the effects of microprocesses on the aggregation behavior. As a result, the parameters affecting the aggregation rate are determined and modeled in the form of a kernel using simple theory of probability and combinations. Because of the random binary collisions of particles in the MC, the modeled kernel is dependent only on the aggregation efficiency term $\beta_0(t)$. Furthermore, it is observed that the kernel, that is, $\beta_0(t)$, and hence the whole aggregation process, has a direct correlation with the total number of particles $N_{p,tot}$, the total number of wet particles $N_{p,wet}$, the collision frequency per particle f_c, the average wet surface coverage fraction per wet particle, and an overall success fraction ψ accounting for the dissipation of kinetic energy. To reflect the effect of process conditions and material properties in the kinetic aggregation model, it was inevitable to model these variables independently. Hence, models for $N_{p,tot}$, $N_{p,wet}$, and the total number of droplets N_{drop} have been developed and discussed under the assumptions and simplifications of CVMC. The three differential equations for $N_{p,tot}$, $N_{p,wet}$, and N_{drop} along with an algebraic equation for the aggregation kernel and a conventional 1-D PBE for pure agglomeration are then

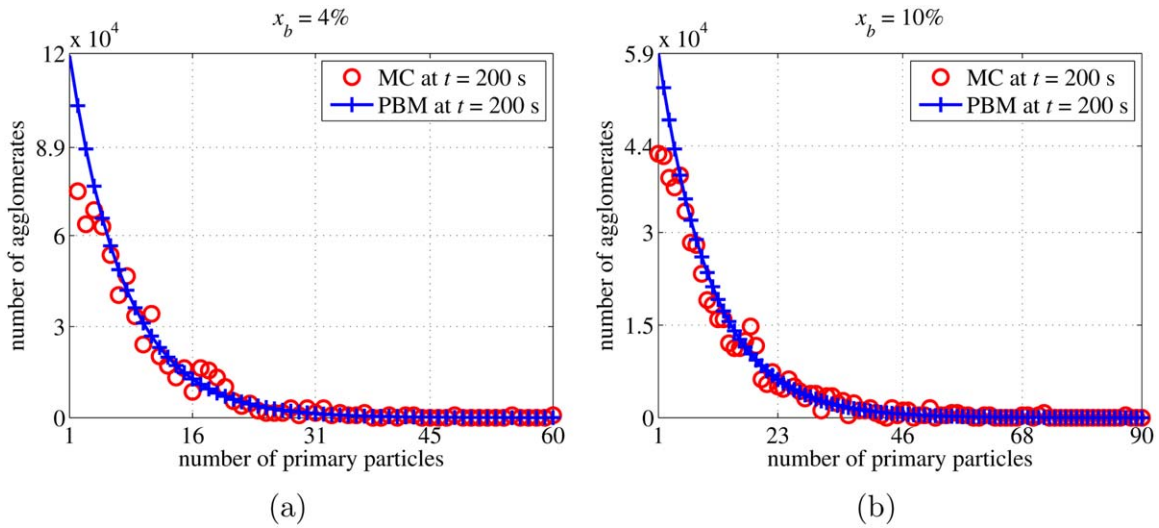

Figure 12. PSDs at $t = 200$ s predicted from simulations of Set-B: (a) MC-04, PBM-04 and (b) MC-05, PBM-05.

[Color figure can be viewed in the online issue, which is available at wileyonlinelibrary.com.]

simultaneously solved by numerical methods to predict the dynamics of the system.

Theoretical validation of the PBM comprising of the Eqs. 1, 13, 14, 26, and 28 was done by comparing the results of PBM with the results of CVMC simulations. Results from two sets of simulations, each set consisting of three simulations by means of MC and PBM, with variations in binder mass flow rate and binder mass fraction were generated and analyzed. The developed technique for simulating the granulation process has shown very encouraging results. In all PBM simulations, almost all predicted results (i.e., $N_{p,tot}$, $N_{p,wet}$, N_{drop}, β_0, and PSD) show a very good match with the corresponding results of MC simulations.

Although PBM has shown good results, the approach can further be improved in many ways. A separate model for binder distribution may be formulated to predict the wet surface coverage fractions at least on a given size of particles. Furthermore, the success fraction concerning the dissipation of kinetic energy ψ should, in principle, be also modeled to make the PBM approach more independent of fitting. Nevertheless, the results presented in this work indicate that values of f_c and ψ can approximately be taken as constants for PBE simulations within a certain window of operating conditions.

The main conclusion of the work is that the effect of process parameters can be modeled in the aggregation kernel, and a microscale method such as MC can play an important role in such study. Furthermore, many variables with distributions at the microscale, such as the average wet surface coverage fraction, can be represented at the macroscale by means of an average value. The proposed model enables to predict the dynamics of SFBG in an improved, providing more information than conventional methods with a relatively low computational effort. Despite of some limitations in the developed technique, the model has illustrated its value and generality by predicting results comparable to MC results for all sets of conducted simulations. This indicates the potential of the developed model to capture the effect of variation in the operating conditions and let us expect a good performance even in more general situations.

Acknowledgments

The authors gratefully acknowledge financial support provided by the German Research Association (DFG) in the frame of Graduate School "Micro-Macro Interactions in Structured Media and Particle Systems" and by the Alexander von Humboldt foundation (research fellowship for Jitendra Kumar).

Notation

A = average area, m^2
B = birth rate, s^{-1}
C = combination
d = diameter, m
D = death rate, s^{-1}
e = restitution coefficient
f = frequency per particle, s^{-1}
I = size classes
k = total number of iterations
m = maximum number of primary particles per agglomerate
$\dot{M}$ = mass flow rate, kg/s
n = number density of particles, $1/m^3$
N = number
$\dot{N}$ = number flow rate, s^{-1}
$\tilde{N}$ = reduced number
P = probability
$\bar{P}$ = system pressure, Pa
$P*$ = saturation pressure, Pa
t = time, s
T = temperature, °C
Δt = time step in Monte-Carlo, s
u = velocity, m/s
v, v' = sizes (volumes) of particles, m^3
x = mass fraction
Y = moisture content, kg/kg
$\tilde{y}$ = molar fraction of vapor

Subscripts

a = asperities
adhes = adhesion
b = binder
c = collision
drop = droplets
dry = dry
dryng = drying
g = gas
l = liquid
p = particle
pp = primary particle
s = successful
tot = total
wet = wet
wd = wet-dry
ww = wet-wet

Superscripts

agg = aggregation
crit = critical
dist = distribution
in = inlet

Abbreviations

CNMC = constant number Monte-Carlo
CVMC = constant volume Monte-Carlo
MC = Monte-Carlo
PSD = particle size distribution
PBE = population balance equation
PBM = population balance model
SFBG = spray fluidized bed granulation

Greek letters

β = aggregation kernel, m^3/s
β_0 = aggregation efficiency, s^{-1}
β^* = size-dependent part of aggregation kernel, m^3
η = wet surface fraction per wet particle/probability of collision at wet surface in wet-dry collision
η_2 = probability of collision at wet surface/s in wet-wet collision
θ = constant angle of droplet with particle surface, degree
ρ = density, kg/m^3
τ = drying time of a droplet, s
ψ = average success fraction due to dissipation of kinetic energy.

Literature Cited

1. Peglow M, Kumar J, Warnecke G, Heinrich S, Mörl L. A new technique to determine rate constant for growth and agglomeration with size- and time-dependent nuclei formulation. *Chem Eng Sci*. 2006;61:282–292.
2. Liu LX, Litster JD. Population balance modeling of granulation with a physically based kernel. *Chem Eng Sci*. 2002;57:2183–2191.
3. Tan HS, Goldschmidt MJ, Boerefijn R, Hounslow MJ, Salman AD, Kuipers JA. Building population balance model for fluidized bed melt granulation: lessons from kinetic theory of granular flow. *Powder Technol*. 2004;142:103–109.
4. Adetayo AA, Litster JD, Pratsinis SE, Ennis BJ. Population balance modelling of drum granulation of materials with wide size distribution. *Powder Technol*. 1995;82:37–49.
5. Adetayo AA, Ennis BJ. Unifying approach to modeling granule coalescence mechanism. *AIChE J*. 1997;43:927–934.
6. Friedlander SK. *Smoke, Dust, and Haze. Fundamentals of Aerosol Dynamics*, 2nd ed. New York: Oxford University Press, 2000.

7. Randolph AD, Larson MA. *Theory of Particulate Processes*, 2nd ed. New York: Academic Press, 1988.
8. Hulburt HM, Katz S. Some problems in particle technology: a statistical mechanical formulation. *Chem Eng Sci.* 1964;19:555–574.
9. Sastry KVS. Similarity size distribution of agglomerates during their growth by coalescence in granulation or green pelletization. *Int J Mineral Process.* 1975;2:187–203.
10. Pearson JMK, Hounslow MJ, Instone T. Tracer studies of high shear granulation, Part 1: population balance modeling. *AIChE J.* 2001;47: 1984–1999.
11. Abberger T. Population balance modeling of granulation. In: Salman AD, Hounslow MJ, Seville JPK, editors. Handbook of Powder Technology. Oxford, UK: Elsevier, 2006:1110–1182.
12. Rajniak P, Stepanek F, Dhanasekharan K, Fan R, Mancinelli C, Chern RT. A combined experimental and computational study of wet granulation in a Wurster fluid bed granulator. *Powder Technol.* 2009;189:190–201.
13. Kapur PC. Kinetics of the granulation by non-random coalescence mechanism. *Chem Eng Sci.* 1972;27:1863–1869.
14. Wauters PAL, Scarlett B, Liu LX, Litster JD, Meesters GMH. A population balance model for high shear granulation. *Chem Eng Sci.* 2002;190:1309–1334.
15. Adetayo AA, Ennis BJ. A new approach to modeling granulation processes for simulation and control purposes. *Powder Technol.* 2000;108:202–209.
16. Ouchiyama N, Tanaka T. The probability of coalescence in granulation kinetics. *Ind Eng Chem Process Des Dev.* 1975;14:286–289.
17. Hussain M, Kumar J, Peglow M, Tsotsas E. Modeling spray fluidized bed aggregation kinetics on the basis of Monte-Carlo simulation results, *Chem Eng Sci.* 2013;101:35–45.
18. Terrazas-Velarde K, Peglow M, Tsotsas E. Stochastic simulation of agglomerate formation in fluidized bed spray drying: a micro-scale approach. *Chem Eng Sci.* 2009;64:2631–2643.
19. Terrazas-Velarde K, Peglow M, Tsotsas E. Investigation of the kinetics of fluidized bed spray agglomeration based on stochastic method. *AIChE J.* 2011a;57:3012–3026.
20. Terrazas-Velarde K, Peglow M, Tsotsas E. Kinetics of fluidized bed spray agglomeration for compact and porous particles. *Chem Eng Sci.* 2011b;66:1866–1878.
21. Kariuki WIJ, Freireich B, Smith RM, Rhodes M, Hapgood KP. Distribution nucleation: quantifying liquid distribution on the particle surface using the dimensionless particle coating number. *Chem Eng Sci.* 2013;92:134–145.
22. Shah BH, Borwanker JD, Ramkrishna D. Monte-Carlo simulation of microbial population balance growth. *Math Biosci.* 1975;31:1–13.
23. Smith M, Matsoukas T. Constant-number Monte-Carlo simulation of population balances. *Chem Eng Sci.* 1998;53:1777–1786.
24. Liffman K. A direct simulation Monte-Carlo method for cluster coagulation. *J Comput Phys.* 2001;100:116–127.
25. Lin Y, Lee K, Matsoukas T. Solution of the population balance equation using constant-number Monte-Carlo. *Chem Eng Sci.* 2002; 57:2241–2252.
26. Dernedde M, Peglow M, Tsotsas E. Stochastic modeling of fluidized bed granulation: influence of droplet pre-drying. *Chem Eng Technol.* 2011;34:1177–1184.
27. Dernedde M, Peglow M, Tsotsas E. A novel, structure-tracking Monte Carlo algorithm for spray fluidized bed agglomeration. *AIChE J.* 2012;58:3016–3029.
28. Metropolis N, Ulam S. The Monte Carlo method. *J Am Stat Assoc.* 1949;44:335–341.
29. Shah BH, Ramkrishna D, Borwanker JD. Simulation of particulate systems using the concept of the interval quiescence. *AIChE J.* 1977;23:897–904.
30. van Peborgh Gooch JR, Hounslow MJ. Monte Carlo simulation of size-enlargement mechanisms in crystallization. *AIChE J.* 1996;42: 1864–1996.
31. Ramkrishna D. *Population Balances: Theory and Applications to Particulate Systems in Engineering*. New York: Academic Press, 2000.
32. Ennis BJ, Tardos G, Pfeffer R. A microlevel-based characterization of granulation phenomena. *Powder Technol.* 1991;65:257–272.
33. Hounslow MJ, Ryall RL, Marshall VR. A discretized population balance for nucleation, growth and aggregation. *AIChE J.* 1988;34: 1821–1832.
34. Bramley AS, Hounslow MJ, Ryall RL. Aggregation during precipitation from solution: a method for extracting rates from experimental data. *J Colloid Interface Sci.* 1996;183:155–165.

Manuscript received July 23, 2013, and revision received Dec. 4, 2013.